



Direct conversion of xylose to furfuryl alcohol on single organic–inorganic hybrid mesoporous silica-supported catalysts

Simone J. Canhaci^{a,b}, Rafael F. Perez^{a,b}, Luiz E.P. Borges^b, Marco A. Fraga^{a,b,*}

^a Instituto Nacional de Tecnologia/MCTIC, Laboratório de Catálise, Av. Venezuela, 82, sala 518, Centro, Rio de Janeiro/RJ 20081-312, Brazil

^b Instituto Militar de Engenharia, Praça Gen. Tibúrcio, 80, Urca, Rio de Janeiro/RJ 22290-270, Brazil



ARTICLE INFO

Article history:

Received 4 October 2016

Received in revised form 13 January 2017

Accepted 31 January 2017

Available online 4 February 2017

Keywords:

Hemicellulose

Pentose

Sugar

Carbohydrate

Saccharide

Sustainable chemistry

ABSTRACT

One-step conversion of xylose to furfuryl alcohol was investigated over Pt catalysts supported on ordered mesoporous SBA-15 bearing $-\text{SO}_3\text{H}$ acid groups. Samples were characterized by SAXRD, FTIR, ^{29}Si CP-NMR, XRF, FE-SEM and TG-MS, and they were all tested in aqueous-phase conversion of xylose in a semi-batch reactor. It was found that the presence of acid sites enhances catalytic activity, confirming that they are also playing a role in xylose conversion. A coupled activity of both metal and acid surface centres was thus suggested. The distribution of products was also found to be significantly modified by grafting organosulfonic groups on catalyst surface; while xylitol was the main product on unmodified Pt/SBA-15 catalyst (selectivity of 45%), a remarkable selectivity of 83–87% to furfuryl alcohol was accomplished over the catalysts supported on organic–inorganic hybrid mesoporous silica. Additionally, no furfural was detected along the aqueous-phase reaction, evidencing that no remote surface acid sites were playing a sole role. It was suggested that direct highly chemoselective conversion of xylose to furfuryl alcohol takes place on vicinal acid–metal surface sites. Finally, the hybrid catalysts were found to be stable regarding their mesostructure framework upon aqueous-phase processing but acid groups resistance to leaching is still the major challenge for one-pot conversion.

© 2017 Elsevier B.V. All rights reserved.

1. Introduction

Lignocellulosic biomass is a valuable renewable feedstock, which is largely available worldwide and comes from a wide variety of sources, mostly agroindustrial and forestry residues such as corn, wheat and rice straws and sugarcane bagasse and straw. These are all by-products of active industrial sectors whose relevance for a country economy depends on its production profile. In Brazil, where ethanol replaces about 40% of gasoline [1] due to the extensive use of flex fuel cars, the agroindustry of sugarcane is a quite significant activity. Nowadays, over 300 sugarcane-processing units are operating in Brazil and they are able to process around 650 million tonnes of sugarcane per year [2], which leads to considerable amounts of lignocellulosic residues (~30 wt.%).

The ever-growing Brazilian demand for ethanol, which is currently used as a biofuel and a platform molecule for industrial production of green chemicals [3], drives the use of cellulose fraction in that abundant biomass to the

biochemical production of second-generation (2G) ethanol. The non-fermentable hemicellulose-derived sugars as well as the lignin fraction from lignocellulosic waste biomass are important sidestreams in 2G ethanol process, which may themselves become a valuable renewable feedstock for green chemicals production. Indeed their conversion into more high added-value compounds in a biofuel integrated production model would provide an additional income, leading to a cost-competitive 2G ethanol.

Hemicellulose is the second-most abundant carbohydrate yielded from fractionation of lignocellulosic biomass, accounting for up to 30% of the total mass. This branched heteropolysaccharide is mainly composed of a mixture of C5 and C6 sugars (pentoses and hexoses), which are easily unlocked by hydrolysis and whose concentration may vary according to the biomass source. However, xylose is the most often primary monosaccharide, which makes it a target molecule to be transformed into alternative biofuels, biofuels additives and biobased products [4,5].

So far, xylose is mostly industrially used to produce furfural from dehydration using mineral acids as homogeneous catalysts [4]. Over the last years, many efforts have been done to develop alternative heterogeneous acid catalysts to establish a more environmentally friendly process [6–8] since furfural is certainly the main industrial chemical produced from hemicellulose. It is indeed

* Corresponding author at: Instituto Nacional de Tecnologia/MCTIC, Laboratório de Catálise, Av. Venezuela, 82, sala 518, Centro, Rio de Janeiro/RJ, 20081-312, Brazil.

E-mail address: marco.fraga@int.gov.br (M.A. Fraga).

reckoned as a key derivative for the production of a wide range of green chemicals as well as a potential biofuel precursor [9,10]. Polymeric resins, heteropolyacids, 3D and 2D zeolites and either functionalized or simple metal oxides have already been exploited as catalysts in this process [6,11–14].

Amongst the furfural-derived industrial chemicals, furfuryl alcohol stands out as 60% of the whole produced aldehyde is consumed for the alcohol production [15]. Furfuryl alcohol is widely used in the manufacturing of chemical resistant furanic resins [13], especially poly(furfuryl alcohol), and a wide range of other chemical intermediates [4,5]. This alcohol is produced from selective hydrogenation of C=O bond of furfural over metal catalysts. Accomplishing chemical selectivity is quite a challenging though as the reduction of C=C bond in the furan ring or the hydrogenation of all C=O and C=C unsaturated bonds of furfural, which may respectively lead to tetrahydrofurfural or tetrahydrofurfuryl alcohol, must be hindered. Copper chromite is the industrially catalyst applied for the gas-phase furfural hydrogenation [16]. The extensive and severe impact of using chromium on the environment and human health has motivated the search for alternative noble metal catalysts, especially Pd [17] and Pt [17–19].

Nevertheless, it has to be outlined that despite whatever novel catalytic systems used either to xylose dehydration or to furfural hydrogenation, furfuryl alcohol would still mandatorily be produced in a two-step process. Furthermore the distinctive catalysts should bear different surface features and operate at distinct conditions, especially temperature, pressure and reaction medium (liquid or gas phase). Some technical difficulties should be overcome to develop a process for the direct conversion of xylose to furfuryl alcohol since many competitive side reactions may occur.

Recently, we have reported the one-pot synthesis of furfuryl alcohol straight from xylose over a dual catalytic system composed of a solid acid (sulfated zirconia, ZrO_2-SO_4) physically mixed with a hydrogenation metal catalyst (Pt/SiO_2) [20]. By adjusting the reaction conditions – temperature and solvent revealing to be the most pertinent variables – and the density of acid and metal catalysts in the dual system, selectivity towards furfuryl alcohol of around 50% could be accomplished. The unprecedented results reported allowed a proof-of-concept and stated the feasibility of establishing a process relying on cascade reactions. Each reaction step proceeding on either catalyst surfaces that are set apart in the liquid phase since the dual system is formed by two separate heterogeneous catalysts [20]. A similar approach was reported by other authors [21], but exploiting a flow-reactor system instead of a batch operation. The use of separate double catalyst bed (an acid catalyst followed by a supported metal catalyst) allowed reaching a remarkable selectivity of 87% to furfuryl alcohol [21].

More lately, we investigated the performance of a single multifunctional catalyst in contrast to the acid/metal dual catalytic system both bearing sulfate groups as acid centres and platinum as metal sites [22]. We could see that setting both sites on the same surface indeed brings some advantages to xylose conversion allowing the straight formation of furfuryl alcohol. The balance between acid and metal sites and their positioning on catalyst surface were found to be crucial to determine product distribution. One-step xylose conversion was suggested to occur on vicinal surface sites. Nevertheless sulfate groups were seen to hydrolyse under reaction conditions leading to acid sites leaching and ultimately to catalyst deactivation [22].

In this contribution, the design of a more chemically-stable single catalyst for one-step conversion of xylose to furfuryl alcohol is further pursued. In the present approach the features of each required surface sites were taken into consideration to develop a single multifunctional hybrid catalyst. The disposal of more resistant active acid centres and the metal sites on the same surface was investigated by designing organo-functionalized mesoporous

silica-supported catalysts. Tailoring the arrangement of the surface centres on the catalyst allowed remarkable chemoselectivity to furfuryl alcohol.

2. Experimental

2.1. Synthesis of organic–inorganic hybrid mesoporous catalysts

SBA-15 was firstly synthesized from tetraethylorthosilicate, TEOS (Sigma–Aldrich), as silicon precursor and poly(ethylene glycol)-block-poly(propylene glycol)-block-poly(ethylene glycol) symmetric triblock copolymer (Pluronic P123), molecular weight = 5800 g/mol – EO₂₀PO₇₀EO₂₀ (Sigma–Aldrich) as template, according to a procedure previously described by Yang et al. [23,24]. Firstly, 2 g of Pluronic P123 was dissolved in 15 g of deionized water and subsequently mixed with a 2 mol/L HCl aqueous solution at room temperature. The final homogeneous solution was heated to 40 °C and then 15.4 g of TEOS was added dropwise under vigorous stirring. The solution was kept under stirring at 40 °C for 20 h. After, it was filtered and the retained white powder was extensively washed with deionized water. It was next suspended in 60 g of H₂O₂ (30 wt.%), transferred to Teflon-lined stainless steel autoclave and hydrothermally treated at 110 °C for 24 h. The synthesized solid was finally filtered, copiously washed with deionized water followed by ethanol and calcined at 500 °C for 5 h following a linear heating rate of 1 °C/min.

A sulfonic-functionalized SBA-15 sample was prepared by grafting, following a post-synthetic functionalization procedure. Initially, thiol surface groups were anchored on silica surface by using 3-mercaptopropyltrimethoxysilane, MPTMS (Sigma–Aldrich) as precursor. In a typical procedure [25], pre-synthesized SBA-15 (1 g) was suspended in organic solution containing 20 mL of xylene and 24.7 g of MPTMS and refluxed for 14 h. Afterwards the powder was filtered, washed with hexane and dried at 100 °C. This organofunctionalized support was then oxidized at room temperature by suspending it in a solution with 10 mL of H₂O₂ (30 wt%) and 20 mL of methanol for 20 h. The powder was recovered by centrifugation, washed with ethanol and submitted to a final complementary oxidation step with a 0.1 mol/L H₂SO₄ aqueous solution. A volume of acid solution to mesoporous powder ratio of 100 mL/g was used. This suspension was remained for 20 h at room temperature under static conditions. Lastly, the powder was once again recovered by centrifugation and washed with ethanol. Propylsulfonic-functionalized sample was labelled as SBA-15-SO₃H.

Finally, the metal-supported catalysts were obtained by incipient wetness impregnation using a H₂PtCl₆ (Sigma–Aldrich) aqueous solution at a concentration to lead to catalysts with different metal loadings and acid/metal molar ratios. The supported samples were dried overnight at 100 °C and calcined in a synthetic air (20 vol%O₂/N₂) stream at 50 mL/min for 4 h at 200 °C, following a heating rate of 10 °C/min. After calcination the catalysts were activated by reduction at 200 °C under a pure hydrogen flow (50 mL/min) for 1 h. Samples were labelled as Pt/SBA-15-SO₃H (x), where x stands for the acid/metal molar ratio.

2.2. Physicochemical characterization

Small-angle X-ray powder diffraction (SAXRD) of all samples was performed using a Bruker D8 Advance with DaVinci design diffractometer equipped with a Lynx-eye position sensitive detector. Analyses were carried out with CuK α radiation in the angular range 0.5°–5° 2θ at a rate of 2°/min.

Porosity was assessed by collecting nitrogen adsorption–desorption isotherms at –196 °C in a Micromeritics ASAP 2020

equipment. Prior to the analysis, the calcined samples were degassed at 150 °C. Specific surface areas were determined by B.E.T. equation and the pore size distribution and the average pore size were obtained using the B.J.H. method using the adsorption branch.

Structural short-range order of silica framework was examined by Fourier transformed infrared spectra (FTIR). The spectra were obtained from 4000 to 400 cm⁻¹ on a Nicolet 6700 Thermo Scientific spectrometer in KBr wafers (3 wt.%) with a resolution of 4 cm⁻¹ and the accumulation of 32 scans.

Local organization was evaluated by ²⁹Si solid state crossed polarization nuclear magnetic resonance (CP-NMR). The ²⁹Si-CP-NMR spectra of all samples were collected in a Bruker 400 Advance II+ spectrometer at a frequency of 79.4 MHz, pulse length of 6 μs and repetition time of 60 s.

Chemical composition was determined by X-ray fluorescence spectrometry (XRF) on a Bruker S8 Tiger spectrometer.

The morphology of SBA-15 samples was examined by field emission scanning electron microscopy (FE-SEM) in a Quanta FEG 450 FEI microscope operating with an accelerating voltage of 20 kV. The samples were spread on metal stubbs and a carbon film was deposited on it before FE-SEM examination.

Thermal stability of organofunctionalized samples was investigated by thermogravimetry in a TA Instruments SDT Q600. Samples were heated up to 1000 °C at a linear rate of 20 °C/min under a synthetic air stream at 30 mL/min. Gaseous products originated from decomposition were analysed in an Ametek Dymaxion quadrupolar mass spectrometer coupled on-line (TG-MS). Signals at m/z = 18, 44, 48, and 64, related to H₂O⁺, CO₂⁺, SO⁺ and SO₂⁺ were concomitantly recorded.

2.3. Catalytic activity

Catalytic performance was examined in the liquid phase in a semi-batch autoclave reactor. The catalysts were previously reduced for 1 h under a hydrogen stream (50 mL/min) at 200 °C, following a linear heating rate of 10 °C/min. Reactions were performed at 130 °C and constant agitation of 600 rpm. In a typical batch, 80 mL of a xylose solution at 83 mmol/L prepared in water:isopropanol (1:1) as solvent was used. Hydrogen was admitted into the reactor and the total pressure was kept constant at 30 bar.

Reactions were carried out for 6 h and samples were taken periodically and analysed by high performance liquid chromatography (HPLC) to determine xylose conversion and product distribution on a molar basis: Conversion of xylose (X_{xy}) = $\frac{[xylose]_i - [xylose]_f}{[xylose]_i} \times 100$; Selectivity (S) = $\frac{[product]}{[xylose]_i - [xylose]_f} \times 100$

Liquid phase aliquots were analysed on a Waters Alliance e2695 liquid chromatograph coupled to a photodiode array detector (PDA) and a refractive index detector (RID). Isocratic HPLC runs were conducted in a Biorad Aminex HPX-87H ion exchange column using an aqueous solution of H₂SO₄ at 5 mmol/L as mobile phase (0.7 mL/min). The temperatures of the column and RID were maintained, respectively, at 65 °C and 50 °C [20,22].

Reusability of the catalyst was evaluated by performing three sequential reaction cycles. After each cycle of 6 h, the reaction liquid was drawn off and another fresh xylose solution (83 mmol/L) in water-isopropanol (1:1) was loaded in. The reactor was purged and finally pressurized with hydrogen to maintain a total pressure of 30 bar. All reaction cycles were carried out at 130 °C.

3. Results and discussion

The effectiveness of SBA-15 synthesis and its post-synthetic organo-functionalization to generate surface acid sites were assessed by examining their long and short-range order, local organization, porosity and morphology. All results and a detailed

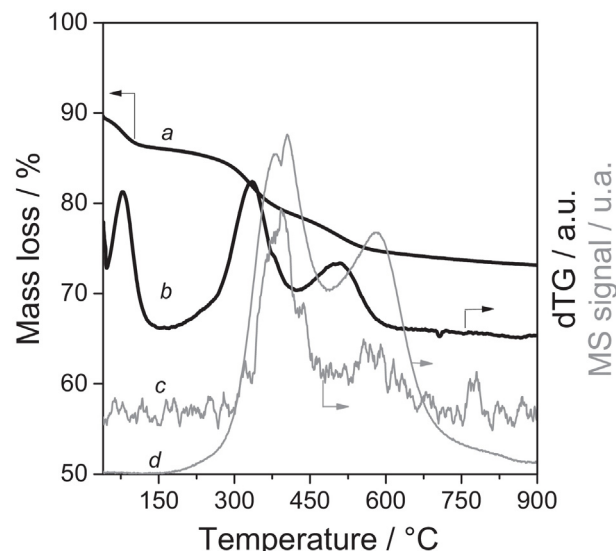


Fig. 1. TG-MS profiles of organofunctionalized SBA-15 samples: (a) TG curve, (b) dTG curve, (c) SO₂ evolution and (d) CO₂ evolution.

discussion are presented as a [Supplementary material](#). Briefly, diffraction patterns ([Figure S1](#)) indicated the formation of a SBA-15 ordered hexagonal mesostructure [12,26]. It was also seen that organic functionalization step induced some loss of long-range organization of SBA-15 framework. N₂ sorption and the adsorption/desorption isotherms ([Figure S2](#)) also confirmed the synthesis efficiency and preservation of the ordered 2D mesoporous structure after its post-synthetic functionalization. As expected, surface area (S_{BET}) and pore volume (V_p) decreased after anchoring of sulfonic acid groups in the framework channels ([Table S1](#)) [12,23,25,27].

Structural short-range order was examined by FTIR ([Figure S3](#)) and all absorptions bands assigned to Si—O—Si units, the existence of double rings and silanol groups (Si—OH) in the solid structure were verified [12,28–30]. No significant difference was observed in the framework-related bands of the post-synthetic functionalized samples ([Figure S3](#)).

Local organization of silicon atoms was investigated by ²⁹Si CP-NMR ([Figure S4](#)) and the Q₄, Q₃ and Q₂ resonances of silicate groups in silica framework were detected. New resonance signals deriving from T₂ and T₃ sites confirmed the covalent linkage between propylsulfonic groups to SBA-15 surface upon post-synthesis grafting ([Figure S4](#)) [12,23].

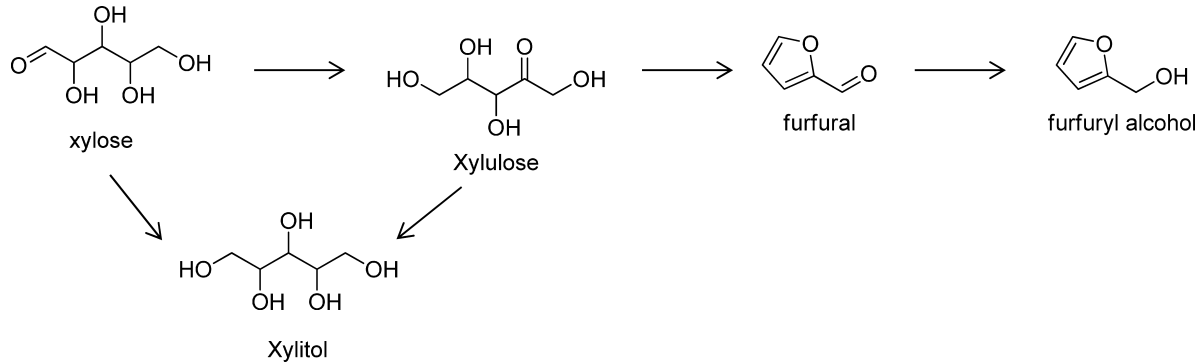
The thermal stability of the organo-functional groups was evaluated using thermogravimetric analysis coupled to a mass spectrometer (TG-MS). Three mass loss events are seen in the SBA-15-SO₃H thermogram ([Fig. 1](#), curves a and b). The first one at low temperature (<150 °C) is associated with sample dehydration (water loss). The other two thermal events occur at 334 °C and 505 °C and are attributed to the decomposition of propylsulfonic surface groups. Indeed, matching CO₂ and sulfur dioxide MS profiles were recorded as displayed in [Fig. 1](#), curves c and d. This finding allowed us to tune the catalyst reduction conditions under which the surface acid sites would be preserved.

All catalysts were then reduced at 200 °C and tested in the transformation of xylose into furfuryl alcohol in liquid phase. A simplified reaction network is presented in [Scheme 1](#). Catalytic runs were performed under hydrogen pressure, at 130 °C using a mixture of water and isopropanol as solvent. It has been previously shown that such reaction conditions do not promote any thermal homogeneous conversion of xylose [20], allowing the assessment of the intrinsic behaviour of the organic–inorganic hybrid mesoporous silica-supported catalysts. Moreover, the use of isopropanol

Table 1

Global xylose conversion (after 6 h) and selectivity to identified products at 20% conversion.

Entry	Sample	X ^a (%)	Selectivity (%)				C ^b (%)
			Xylitol	Xylulose	Furfural	Furfuryl alcohol	
1	Pt/SBA-15	34	46	54	0	0	92
2	Pt/SBA-15-SO ₃ H (12)	65	2	15	0	83	91
3	Pt/SBA-15-SO ₃ H (20)	56	1	12	0	87	100
4	Pt/SBA-15-SO ₃ H (28)	44	3	10	1	86	100

^a Conversion of xylose after 6 h.^b Carbon balance at 20% conversion.**Scheme 1.** Simplified reaction network of xylose conversion to furfuryl alcohol.

as co-solvent in this system pressurized with molecular hydrogen was shown to bring no significant contribution to the formation of hydrogenated products *via* transfer hydrogenation (MPV reduction) [22].

A control experiment was firstly conducted with an unmodified SBA-15-supported Pt catalyst (Pt/SBA-5) to unveil the eventual role played by the surface acid sites on the hybrid samples. Catalytic performance and the time-dependent concentration profiles are presented in Table 1 (entry 1) and Fig. 2A, respectively.

Xylose conversion of around 34% is reached over this sample after 6 h, indicating that it is certainly an active catalyst as it could be expected. Nonetheless, only xylulose and xylitol are formed, which discloses that xylose isomerization to its ketopentose form and sugar hydrogenation to its polyhydric alcohol are the only reactions taking place. Typical hydrogenation activity of Pt metal sites is clear by the high selectivity to xylitol at isoconversion conditions (~20%) as summarized in Table 1 (entry 1). Xylose isomerization, on the other hand, occurs on weak Lewis acid sites on SBA-15 as confirmed by a control experiment performed with a metal-free SBA-15 sample. Despite the very low activity (conversion of xylose < 7%), the ketopentose was the major product identified in this blank run, with a minor formation of furfural. A similar behaviour was indeed reported before on a bare commercial silica sample [20]. An examination of concentration curves (Fig. 2A) reveals that xylulose acts like an intermediate in the way to sugar reduction.

The behaviour of a parent catalyst supported on SBA-15 bearing propylsulfonic acid groups (Pt/SBA-15-SO₃H(12)) is completely different though. An increase in global catalytic activity is seen from xylose concentration profile depicted in Fig. 2B, which leads to a sugar conversion of 65% after 6 h (Table 1, entry 2). This finding noticeably shows that the acid sites are indeed playing a role in xylose conversion and a coupled activity of both metal and acid surface centres can be suggested. As a matter of fact, we have previously reported a similar contribution of acid sites on sugar transformation when a dual acid/metal catalytic system was applied [20]. Nevertheless, one should bear in mind that in our earlier study [20] acid and metal sites were settled onto different surfaces in a dual system (physical mixtures) and thus

independent cascade or side reactions were allowed to proceed. Indeed we reported on the occurrence of polymerization and condensation reactions producing high molecular weight compounds [20]. In the present work, the results indicate that disposing acid sites along with metal centres on the same catalyst surface also renders much more active systems. Additionally, a better reaction control may be accomplished as a satisfactory carbon balance was reached along all experiments as collected in Table 1.

The distribution of products is also found to be significantly modified by grafting organosulfonic groups on catalyst surface as shown in Fig. 2B. Only a minor formation of xylulose and xylitol is registered and the major product identified is now furfuryl alcohol, reaching an outstanding selectivity of 83% at ~20% isoconversion level (Table 1, entry 2). To the best of our knowledge, it is indeed the highest selectivity to furfuryl alcohol ever accomplished through direct conversion of xylose on a single heterogeneous catalyst.

Time-dependent selectivity trends depicted in Fig. 3 imply once again that even though xylulose is formed, it is converted along reaction, playing thus an intermediate role in aldopentose catalytic transformation. By comparing the patterns obtained for Pt/SBA-15 (Fig. 3A) and Pt/SBA-15-SO₃H (12) (Fig. 3B), it is clear that straightforward xylose/xylulose hydrogenation to xylitol is severely hindered when acid sites are added to catalyst surface, suggesting the absence of isolated metal sites on this sample. Furthermore, it must be outlined that no furfural was detected whatsoever along the whole experiment (Fig. 3B) contrarily to what was observed before over a physical mixture of acid and metal catalysts [20] or a single catalyst supported on sulphated ZrO₂ [22]. It suggests that no remote surface acid sites are playing a sole role either. Moreover, it points to the conclusion that a more uniform distribution of acid sites on catalyst surface must be achieved to provide a highly selective catalyst and it can be accomplished by using a mesoporous ordered support.

However, due to the clear differences between the catalytic system reported elsewhere (sulfated zirconia-supported catalyst) [22] and the one investigated herein (sulfonic acid functionalized SBA-15 materials), particularly their acid strength and texture, a physical mixture of Pt/SBA-15 and SBA-15-SO₃H was also tested in

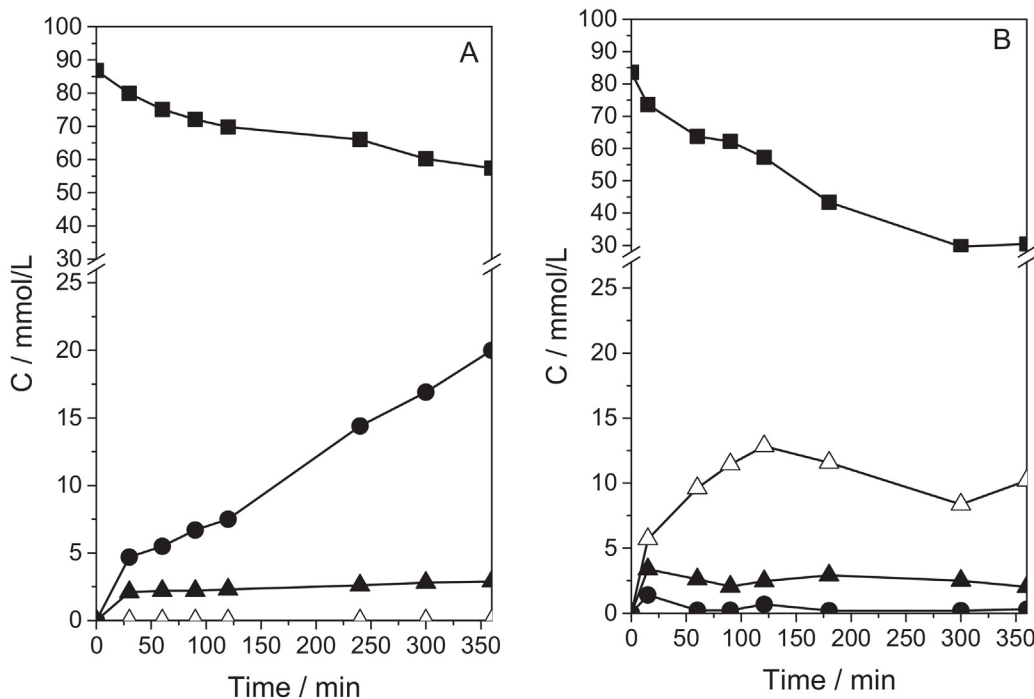


Fig. 2. Time-dependent concentration profiles for (A) Pt/SBA-15 and (B) Pt/SBA-15-SO₃H (12): xylose (■); xylitol (●); xylulose (▲); furfuryl alcohol (△).

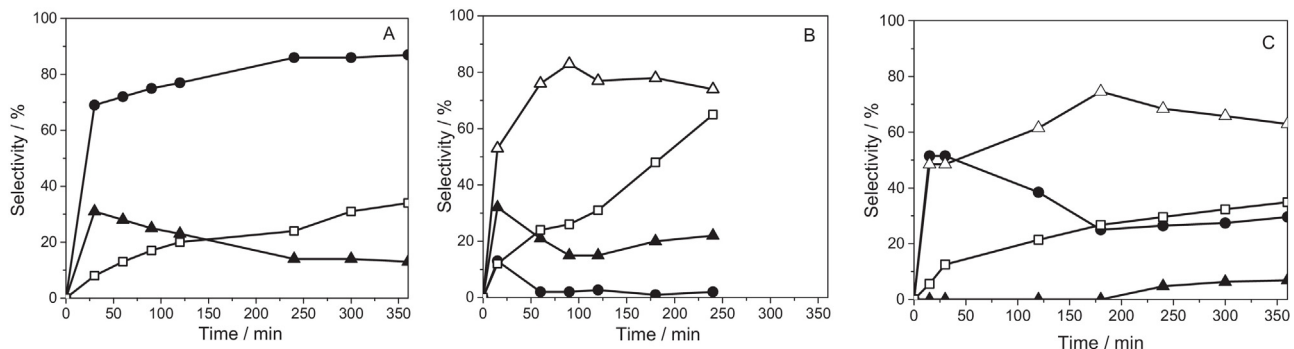


Fig. 3. Time-dependent selectivity and xylose conversion for (A) Pt/SBA-15, (B) Pt/SBA-15-SO₃H (12) and (C) Pt/SBA-15 + SBA-15-SO₃H: xylose conversion (□); xylitol (●); xylulose (▲); furfuryl alcohol (△).

this study. As seen in Fig. 3C, some differences on product distribution are revealed when compared to the performance of the single Pt/SBA-15-SO₃H catalyst (Fig. 3B). Furfuryl alcohol is still the major product but the formation of xylitol is much more significant most likely due to the straight hydrogenation of xylose on free Pt/SBA-15.

All together, these findings finally lead us to the conclusion that direct chemoselective conversion of xylose to furfuryl alcohol indeed takes place on vicinal acid–metal surface sites. In such mechanism, xylose is dehydrated on sulfonic acid groups to intermediate furfural adsorbed species, which is then directly reduced to the corresponding unsaturated alcohol over the metal sites. Only after these sequential surface reaction steps occur that the end product is desorbed to the liquid-phase reaction medium. These results are in very good agreement with the reaction model we suggested previously for low-selective sulfated-zirconia-based multifunctional catalysts [22].

Further experimental evidences were taken by synthesizing two more samples bearing different acid/metal site ratios, Pt/SBA-15-SO₃H (20) and Pt/SBA-15-SO₃H (28). Time-dependent concentration profiles and catalytic performance are presented in Fig. 4 and Table 1 (entries 3 and 4), respectively. A similar reaction

dynamics was found – harsh inhibition of monosaccharide direct hydrogenation to its polyhydric alcohol, negligible sole sugar dehydration to furfural and an expressive formation of furfuryl alcohol, corroborating the interplay between acid and metal sites disposed on hybrid catalyst surface.

To infer on catalyst stability, particularly on the preservation of their hierarchical mesoporous framework and leaching-resistance of sulfonic acid groups, the catalysts were recovered by filtration after reaction, copiously washed with deionized water, dried overnight and examined by SAXRD and XRF. No significant change was seen on SAXRD pattern or on Pt loading (Table 2), confirming that noble metals are stable enough to be applied in aqueous-phase processing of biomass-derived second-generation sugars. Sulfur content, on the other hand, was seen to drop and this decrease was more relevant the higher the sulfur concentration in the fresh catalyst (Table 2). Nevertheless, this performance surpasses that reported elsewhere regarding poorly stable multifunctional catalysts holding sulfate acid groups instead [22]. It is likely attributed to the higher tolerance of $-\text{SO}_3\text{H}$ groups to hydration due to the covalent bonding of such groups on the surface of ordered mesoporous silica [31,32].

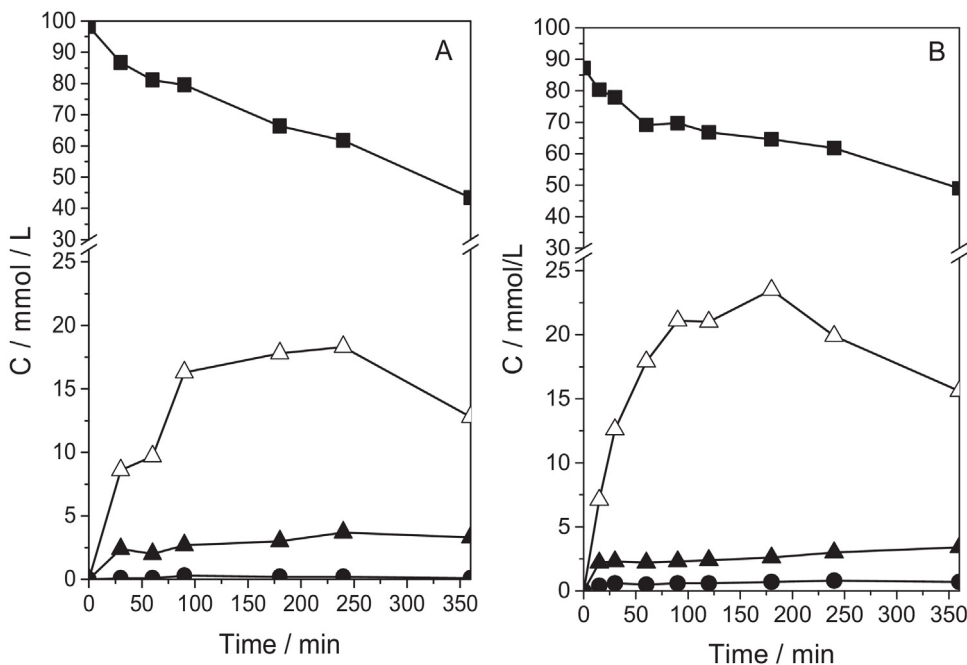


Fig. 4. Time-dependent concentration profiles for (A) Pt/SBA-15-SO₃H (20) and (B) Pt/SBA-15-SO₃H (28): xylose (■); xylitol (●); xylulose (▲); furfuryl alcohol (△).

Table 2
Chemical composition of fresh and spent catalysts.

Sample	Fresh catalyst			Spent catalyst		
	[Pt] (mmol/g)	[S] (mmol/g)	Acid/metal molar ratio	[Pt] (mmol/g)	[S] (mmol/g)	Acid/metal ratio
Pt/SBA-15	0.057	—	0	0.056	—	0
Pt/SBA-15-SO ₃ H (12)	0.056	0.688	12	0.056	0.563	10
Pt/SBA-15-SO ₃ H (20)	0.031	0.625	20	n.d.	n.d.	n.d.
Pt/SBA-15-SO ₃ H (28)	0.046	1.281	28	0.046	0.819	18

n.d., not determined.

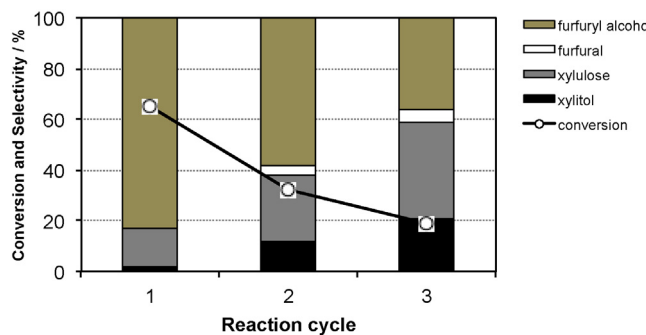


Fig. 5. Evolution of xylose conversion and selectivities of products after each reaction cycle performed with Pt/SBA-15-SO₃H (12) catalyst.

Catalyst reusability was also evaluated by performing three sequential reaction cycles with Pt/SBA-15-SO₃H (12) sample and the results concerning xylose conversion and selectivity of all products are depicted in Fig. 5.

It is seen that global activity decreases after each reaction cycle, reaching a xylose conversion level of around 20% after the third sequential run. Product distribution changes likewise. Even though furfuryl alcohol is always produced as the major product, formation of xylitol from direct hydrogenation of xylose as well as sugar isomerization on Lewis acid sites are gradually observed after every cycle. It indicates some deactivation of Brønsted acid sites, which are well reckoned as responsible for xylose dehydration [33]. This

trend is in close agreement with the steady loss of sulfur content as discussed previously (Table 2), since it is a direct assessment of Brønsted acid sites (sulfonic groups), and reveals that leaching of these sites deeply disturbs product distribution.

All in all, this contribution systematically reports that assembling acid and metal centres on the surface of mesostructured silica renders active and selective catalysts for the direct conversion of hemicellulose-derived pentose. Moreover, it corroborates our previously proposed model [22] whereby both acid and metal sites concomitantly play a role in the reaction providing a highly chemoselective catalyst for one-step production of furfuryl alcohol from xylose. Improvement of catalyst stability, however, is still required and it stands as the major challenge for the development of a single multifunctional catalyst for xylose direct conversion.

4. Conclusion

Furfuryl alcohol can be produced directly from xylose in a single step process by using bifunctional metal/acid catalysts. The presence of $-\text{SO}_3\text{H}$ surface acid sites suppresses the hydrogenation of xylose to the corresponding sugar alcohol, leading to the chemoselective hydrogenation of dehydrated-intermediate aldehyde. Sulfonated ordered mesoporous silica-supported catalysts indeed render active and highly selective hybrid systems for production of furfuryl alcohol. Remarkable selectivities within 83–87% were accomplished in the straightforward sugar conversion. Hybrid catalysts were found to be stable as regarding their mesostructure framework upon aqueous-phase processing but acid groups

resistance to leaching is still poor and stands as the major challenge for pentose valorization.

Acknowledgements

The authors are indebted to Prof. Heloise O. Pastore (UNICAMP) for her assistance with the ^{29}Si CP-NMR analyses. Financial support from CNPq and FAPERJ is also acknowledged. SJC and RFP also thank CAPES for their grants.

Appendix A. Supplementary data

Supplementary data associated with this article can be found, in the online version, at <http://dx.doi.org/10.1016/j.apcatb.2017.01.085>.

References

- [1] E.S. Lora, R.V. Andrade, Renew. Sustain. Energy Rev. 13 (2009) 777–788.
- [2] V. Ferreira-Leitão, L.M.F. Gottschalk, M.A. Ferrara, A.L. Nepomuceno, H.B.C. Molinari, E.P.S. Bon, Waste Biomass Valoriz. 1 (2010) 65–76.
- [3] B. Perlatti, M.R. Forim, V.G. Zuin, Chem. Biol. Technol. Agric. 1 (2014) 1–9.
- [4] A. Corma, S. Iborra, A. Velty, Chem. Rev. 107 (2007) 2411–2502.
- [5] J.N. Chheda, G.W. Huber, J.A. Dumesic, Angew. Chem. Int. 46 (2007) 7164–7183.
- [6] A.S. Dias, M. Pillinger, A.A. Valente, J. Catal. 229 (2005) 414–423.
- [7] A.S. Dias, S. Lima, D. Carriazo, V. Rives, M. Pillinger, A.A. Valente, J. Catal. 244 (2006) 230–237.
- [8] A.S. Dias, S. Lima, M. Pillinger, A.A. Valente, Catal. Lett. 114 (2007) 151–160.
- [9] M.J. Climent, A. Corma, S. Iborra, Green Chem. 13 (2011) 520–540.
- [10] J.B. Binder, J.J. Blank, A.V. Cefali, R.T. Raines, ChemSusChem 3 (2010) 1268–1272.
- [11] C. Moreau, R. Durand, D. Peyron, J. Duhamet, P. Rivalier, Ind. Crops Prod. 7 (1998) 95–99.
- [12] X. Shi, Y. Wu, H. Yi, G. Rui, P. Li, M. Yang, G. Wang, Energies 4 (2011) 669–684.
- [13] M.M. Antunes, S. Lima, A. Fernandes, M. Pillinger, M.F. Ribeiro, A.A. Valente, Appl. Catal. A: Gen. 417–418 (2012) 243–252.
- [14] A.S. Mamman, J.-M. Lee, Y.-C. Kim, I.T. Hwang, N.-J. Park, Y.K. Hwang, J.-S. Chang, J.-S. Hwang, Biofuels Bioprod. Biorefin. 2 (2008) 438–454.
- [15] I. Agirrezabal-Tellería, A. Larreategui, J. Requies, M.B. Güemez, P.L. Arias, Bioresour. Technol. 102 (2011) 7478–7485.
- [16] J. Lee, Y. Xu, G.W. Huber, Appl. Catal. B: Environ. 140–141 (2013) 98–107.
- [17] W. Yu, Y. Tang, L. Mo, P. Chen, H. Lou, X. Zheng, Bioresour. Technol. 102 (2011) 8241–8246.
- [18] J. Kijeniski, P. Winiarek, T. Paryjczak, A. Lewicki, A. Mikołajska, Appl. Catal. A: Gen. 233 (2002) 171–182.
- [19] H.A. Rojas, G.B. Guerra, J.J. Murcia, P.R. Nuñez, Sci. Technic 1 (2007) 653–657.
- [20] R.F. Perez, M.A. Fraga, Green Chem. 16 (2014) 3942–3950.
- [21] J. Cui, J. Tan, X. Cui, Y. Zhu, T. Deng, G. Ding, Y. Li, ChemSusChem 9 (2016) 1259–1262.
- [22] R.F. Perez, S.J. Canhaci, L.E.P. Borges, M.A. Fraga, Catal. Today (2016), <http://dx.doi.org/10.1016/j.cattod.2016.09.003>.
- [23] L.M. Yang, Y.J. Wang, G.S. Luo, Y.Y. Dai, Microporous Mesoporous Mater. 84 (2005) 275–282.
- [24] L.M. Yang, Y.J. Wang, G.S. Luo, Y.Y. Dai, Microporous Mesoporous Mater. 81 (2005) 107–114.
- [25] G.H. Jeong, E.G. Kim, S.B. Kim, E.D. Park, S.W. Kim, Microporous Mesoporous Mater. 144 (2011) 134–139.
- [26] D. Zhao, J. Feng, Q. Huo, N. Melosh, G.H. Fredrickson, B.F. Chmelka, G.D. Stucky, Science 279 (1998) 548–552.
- [27] S. Sreevardhan Reddy, B. David Raju, V. Siva Kumar, A.H. Padmasri, S. Narayanan, K.S. Rama Rao, Catal. Commun. 8 (2007) 261–266.
- [28] M. Colilla, I. Izquierdo-Barba, M. Vallet-Regí, Microporous Mesoporous Mater. 135 (2010) 51–59.
- [29] E. Monsivais-Gámez, F. Ruiz, J.R. Martínez, J. Solgel Sci. Technol. 43 (2007) 65–72.
- [30] J. Tu, N. Li, W. Geng, R. Wang, X. Lai, Y. Cao, T. Zhang, X. Li, S. Qiu, Sens. Actuators B: Chem. 166–167 (2012) 658–664.
- [31] S. Suganuma, K. Nakajima, M. Kitano, D. Yamaguchi, H. Kato, S. Hayashi, M. Hara, JACS 130 (2008) 12787–12793.
- [32] X. Wang, R. Liu, M.M. Waje, Z. Chen, Y. Yan, K.N. Bozhilov, P. Feng, Chem. Mater. 19 (2007) 2395–2397.
- [33] V. Choudhary, S.I. Sandler, D.G. Vlachos, Appl. Catal. B 2 (2012) 2022–2028.